

# UC Berkeley

## UC Berkeley Previously Published Works

### Title

Dicopper Cu(I)Cu(I) and Cu(I)Cu(II) Complexes in Copper-Catalyzed Azide-Alkyne Cycloaddition

### Permalink

<https://escholarship.org/uc/item/1p87h7fj>

### Journal

Journal of the American Chemical Society, 139(15)

### ISSN

0002-7863

### Authors

Ziegler, Micah S  
Lakshmi, KV  
Tilley, T Don

### Publication Date

2017-04-19

### DOI

10.1021/jacs.6b13261

Peer reviewed

# Dicopper Cu(I)Cu(I) and Cu(I)Cu(II) Complexes in Copper-Catalyzed Azide–Alkyne Cycloaddition

Micah S. Ziegler,<sup>†,‡</sup> K. V. Lakshmi,<sup>§</sup> and T. Don Tilley<sup>\*,†,‡</sup>

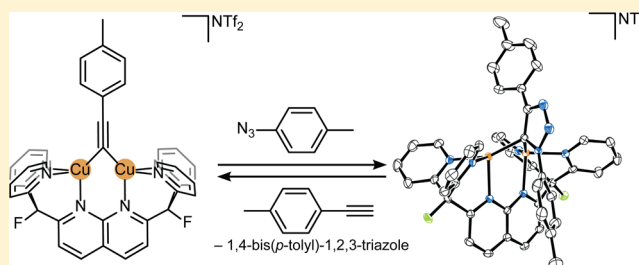
<sup>†</sup>Department of Chemistry, University of California, Berkeley, California 94720-1460, United States

<sup>‡</sup>Chemical Sciences Division, Lawrence Berkeley National Laboratory, Berkeley, California 94720, United States

<sup>§</sup>Department of Chemistry and Chemical Biology and The Baruch '60 Center for Biochemical Solar Energy Research, Rensselaer Polytechnic Institute, Troy, New York 12180, United States

## Supporting Information

**ABSTRACT:** A discrete, dicopper  $\mu$ -alkynyl complex,  $[\text{Cu}_2(\mu\text{-}\eta^1\text{-}\eta^1\text{-C}\equiv\text{C}(\text{C}_6\text{H}_4)\text{CH}_3)\text{DPFN}]\text{NTf}_2$  (DPFN = 2,7-bis(fluoro-di(2-pyridyl)methyl)-1,8-naphthyridine;  $\text{NTf}_2^- = \text{N}(\text{SO}_2\text{CF}_3)_2^-$ ), reacts with *p*-tolylazide to yield a dicopper complex with a symmetrically bridging 1,2,3-triazolide,  $[\text{Cu}_2(\mu\text{-}\eta^1\text{-}\eta^1\text{-}(1,4\text{-bis}(4\text{-tolyl})\text{-}1,2,3\text{-triazolide}))\text{DPFN}]\text{NTf}_2$ . This transformation exhibits bimolecular reaction kinetics and represents a key step in a proposed, bimetallic mechanism for copper-catalyzed azide–alkyne cycloaddition (CuAAC). The  $\mu$ -alkynyl and  $\mu$ -triazolide complexes undergo reversible redox events (by cyclic voltammetry), suggesting that a cycloaddition pathway involving mixed-valence dicopper species might also be possible. Synthesis and characterization of the mixed-valence  $\mu$ -alkynyl dicopper complex,  $[\text{Cu}_2(\mu\text{-}\eta^1\text{-}\eta^1\text{-C}\equiv\text{C}(\text{C}_6\text{H}_4)\text{CH}_3)\text{-DPFN}](\text{NTf}_2)_2$ , revealed an electronic structure with an unexpected partially delocalized spin, as evidenced by electron paramagnetic resonance spectroscopy. Studies of the mixed-valence  $\mu$ -alkynyl complex's reactivity suggest that a mixed-valence pathway is less likely than one involving intermediates with only copper(I).



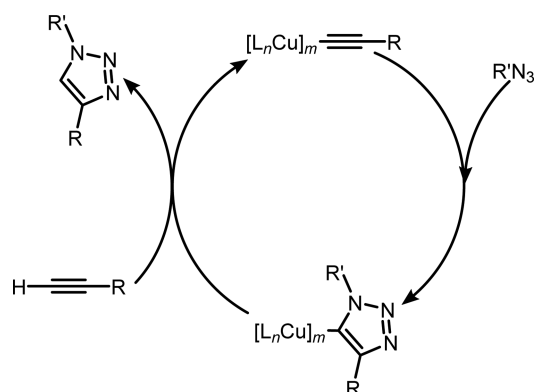
## INTRODUCTION

From initial reports in the 1980s<sup>1,2</sup> and seminal work in the 2000s,<sup>3,4</sup> the copper-catalyzed azide–alkyne cycloaddition (CuAAC) has become renowned for its utility and has found applications in, for example, small-molecule, polymer, and materials syntheses as well as biochemical labeling.<sup>5–18</sup> However, the CuAAC mechanism has resisted elucidation, prompting a range of experimental and theoretical studies.<sup>16,19–31</sup> A general, simplified mechanism of CuAAC under aprotic conditions (Scheme 1) is postulated to include Cu-

bound alkynyl and triazolide intermediates, but the nuclearity of the copper intermediates ( $[\text{L}_n\text{Cu}]_m$ ) is uncertain.<sup>25,27</sup> Notably, experimental investigations of the reaction's mechanism and catalyst nuclearity are often complicated by aggregation of Cu(I) acetylides, commonly into insoluble polymeric materials, and interconversion of catalytic species.<sup>20,24,25,30,32–36</sup> Bases can also introduce complexity by enabling additional protonation and deprotonation steps in the catalytic cycle (omitted for simplicity in Scheme 1).<sup>25,27</sup> More recently, kinetics studies,<sup>20,23,37–39</sup> isotopic copper labeling,<sup>40</sup> mass spectroscopy,<sup>41,42</sup> and isolation of presumed copper intermediates<sup>39,43</sup> suggested the intermediacy of dicopper species in catalysis. Multicopper, and specifically dicopper, catalytic intermediates have also been supported by computational studies.<sup>30,31,44–46</sup>

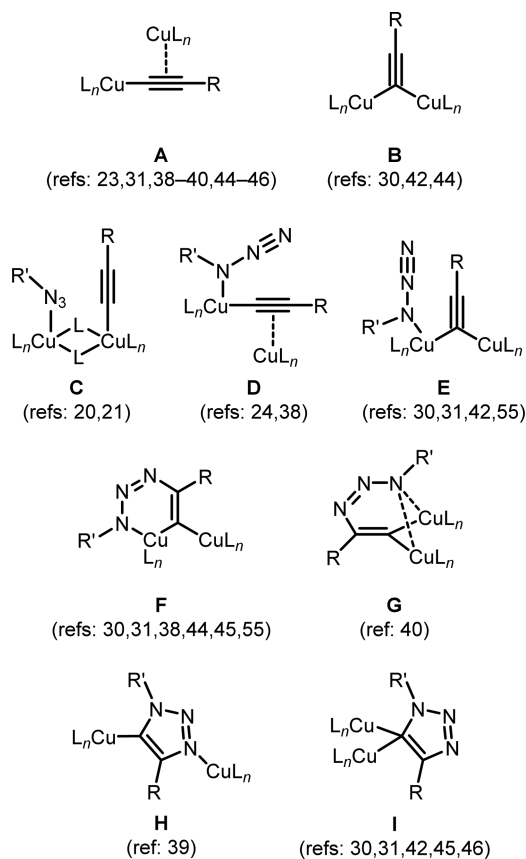
On the basis of these experimental and computational studies, many intermediates (some of which are shown in Chart 1) have been proposed for mechanisms that involve cooperation between two copper centers. Only recently have presumed dinuclear complexes been isolated and shown to undergo discrete steps in a potential CuAAC cycle, notably the transformation of A into H as reported by Jin and co-workers.<sup>39</sup> However, this and other recent reports of proposed CuAAC intermediates have employed systems that potentially allow

Scheme 1. General Scheme of CuAAC in Aprotic Conditions



Received: December 25, 2016

Published: April 10, 2017

Chart 1. Proposed Dinuclear CuAAC Intermediates<sup>a</sup>

<sup>a</sup>Selected references are in parentheses.

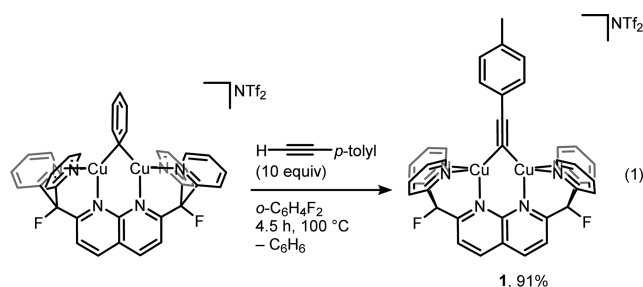
both monocopper and dicopper pathways to operate.<sup>32,39,40</sup> Moreover, intermediate I, while supported computationally,<sup>30,31,45,46</sup> has remained unobserved in these studies. In addition, in nearly all of these cases, the two catalytically active copper centers are presumed to be in the +1 oxidation state even though there is evidence that Cu(II) might accelerate the CuAAC reaction,<sup>37</sup> possibly by playing a role that complements Cu(I).<sup>47</sup>

As described here, the potential for mechanistic pathways that feature dicopper intermediates in the CuAAC reaction has been investigated with the rigid, dinucleating ligand (2,7-bis(fluoro-di(2-pyridyl)-methyl)-1,8-naphthyridine, DPFN) that supports discrete cationic dicopper complexes with bridging hydrocarbyl ligands and mixed-valence electronic states.<sup>48</sup> This work involves synthesis of a  $\mu$ -alkynyl dicopper(I,I) complex and observation of its reaction with an organic azide. This reaction gives a  $\mu$ -triazolide species that is also very likely an intermediate on a CuAAC catalytic cycle. These results therefore provide strong support for the viability of a dicopper mechanism and establish structural information concerning key intermediates in such a cycle. Further investigations have shown that analogous, mixed-valence dicopper(I,II) complexes are much less likely to be active in CuAAC catalysis.

## ■ DICOPPER(I) ALKYNYL COMPLEX

Previous work has shown that a dicopper complex of DPFN abstracts a phenyl group from tetraphenylborate to yield the  $\mu$ -Ph complex  $[\text{Cu}_2(\mu\text{-}\eta^1\text{:}\eta^1\text{-Ph})\text{DPFN}]\text{NTf}_2$  and that the resulting aryl group can be exchanged for  $\text{C}_6\text{F}_5\text{H}$  with concomitant generation of benzene.<sup>48</sup> Analogously, treatment

of the  $\mu$ -phenyl complex with 10 equiv of *p*-tolylacetylene and heating at 100 °C for 4.5 h in *o*- $\text{C}_6\text{H}_4\text{F}_2$  gave elimination of benzene and the bridging alkynyl complex  $[\text{Cu}_2(\mu\text{-}\eta^1\text{:}\eta^1\text{-C}\equiv\text{C}(\text{C}_6\text{H}_4)\text{CH}_3)\text{DPFN}]\text{NTf}_2$  (**1**, eq 1), which was isolated in 91% yield.



The solid-state structure of **1** contains two independent molecules of the dicopper cation in the asymmetric unit (one is shown in Figures 1 and SC1). Both molecules exhibit

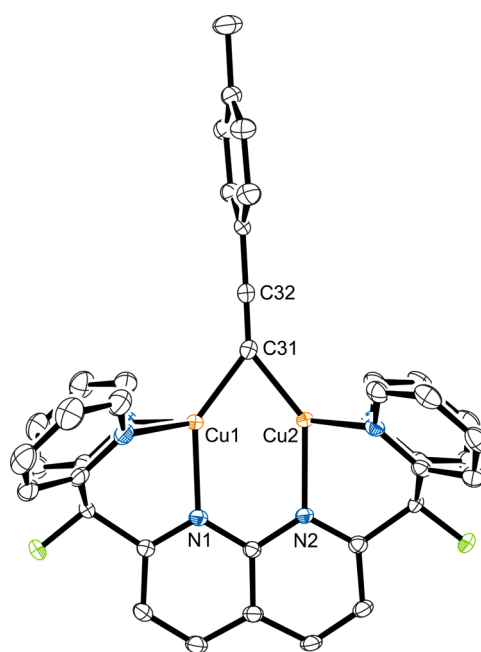


**Figure 1.** Solid-state structure of **1** as determined by single-crystal X-ray diffraction. Only one dicopper cation in the asymmetric unit is shown; the other cation, four  $\text{C}_6\text{H}_5\text{F}$  molecules of solvation, two  $\text{NTf}_2^-$  counterions, and hydrogen atoms are omitted for clarity. Thermal ellipsoids are set at the 50% probability level.

symmetrically bridging *p*-tolylalkynyl ligands; the  $\angle\text{C32-C31-Cu}$  angles are all between 140.9(3) and 143.8(3)°, similar to the  $\angle\text{Cpara-Cipso-Cu}$  angles in the  $\mu$ -Ph complex (144.4(1) and 143.0(1)°), and the Cu–C31 bonds are all in the range of 1.949(3)–1.956(4) Å. The  $^1\text{H}$  NMR spectra of **1** (ca. 10 mM) in  $\text{THF-}d_6$  at 25 °C are consistent with the solid-state structure, suggesting that also in solution, the  $\mu$ -alkynyl ligand symmetrically bridges the copper atoms. This symmetric binding is notable considering the tendency of multicopper alkynyl complexes to bind in a  $\sigma,\pi$ - (i.e.,  $\mu\text{-}\eta^1\text{:}\eta^2$ ) fashion, but is not without precedent.<sup>49,50</sup>

The Cu–C31 distances (average: 1.953(2) Å) are significantly shorter than analogous distances in the  $\mu$ -Ph complex (average: 2.020(1) Å). This difference in Cu–C distances is

consistent with hybridization at carbon and could also result from greater electron donation from the Cu(I) atoms into the alkynyl  $\pi$ -system. This more compact core structure also extends to the Cu...Cu distance; in **1** the average Cu...Cu distance is 2.3885(4) Å, which is shorter than that observed for the  $\mu$ -Ph complex (2.3927(5) Å).

A few other cationic bridging alkynyl copper compounds have been isolated and structurally characterized.<sup>35,39,49–53</sup> Compared to the two structurally characterized dicopper examples reported by Jin and co-workers in their study of CuAAC,<sup>39</sup> the alkynyl moiety in **1** bridges in a significantly more symmetric manner. The binding in **1** is similar to that of a complex synthesized by Kuang et al., [Cu<sub>2</sub>( $\mu$ -L)<sub>2</sub>( $\mu$ - $\eta^1$ : $\eta^1$ -C $\equiv$ CPh)]ClO<sub>4</sub>, where L = 2-(diphenylphosphino)-6-(pyrazol-1-yl)pyridine.<sup>52</sup> However, the Cu...Cu and Cu–C distances in **1** are significantly shorter than corresponding distances in Kuang's complex (2.517(2) Å and 2.045(9), 2.078(8) Å, respectively).

A <sup>1</sup>H–<sup>13</sup>C HMBC experiment slightly modified to allow for couplings as low as  $J_{C-H} \approx 3.5$  Hz was performed on a solution of **1** in THF-*d*<sub>8</sub> at 25 °C and 700 MHz (16.4 T, Figures S1–5). The spectrum revealed six cross peaks correlated with the methyl resonance, suggesting that it reported every carbon in the  $\mu$ -alkynyl ligand's conjugated  $\pi$ -system, including the terminal Cu<sub>2</sub>-bound carbon, which would constitute a <sup>7</sup>J<sub>C-H</sub> observation (Figure 2b). While observation of such a long-

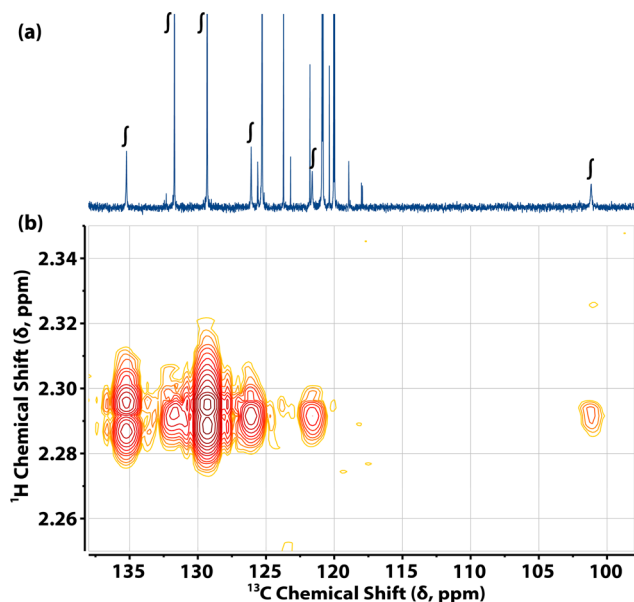


**Figure 2.** <sup>13</sup>C{<sup>1</sup>H} (a) and <sup>1</sup>H–<sup>13</sup>C HMBC (b) NMR spectra, acquired at 21.1 and 16.4 T respectively, of a solution of **1** in THF-*d*<sub>8</sub>. Note that six distinct correlations observed in the HMBC are also observed directly as resonances in the <sup>13</sup>C{<sup>1</sup>H} spectrum, which are denoted with *f*.

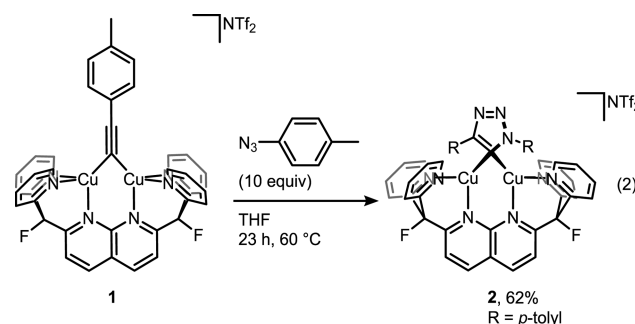
range correlation is unexpected, electronic effects on the chemical shift of a substituted phenylacetylenes's terminal carbon resonance have been observed upon variation of the *para*-substituent.<sup>54</sup> Direct observation of the carbon resonances in **1** was achieved via a 1D <sup>13</sup>C{<sup>1</sup>H} experiment recorded at 900 MHz (21.1 T, 26,624 scans, Figures 2a and S6–7) and confirmed that all six correlations observed in the HMBC experiment correspond to carbon-13 resonances. Combined with a <sup>1</sup>H–<sup>13</sup>C HSQC experiment, these data allow tentative

assignment of the 101.17 ppm resonance as the bridging carbon in the  $\mu$ -alkynyl moiety and the 121.62 ppm resonance as the internal alkynyl carbon. These assignments are consistent with those observed in a recently reported cationic copper cluster containing bridging acetylides.<sup>35</sup>

## SYNTHESIS AND REACTIVITY OF A BRIDGING TRIAZOLIDE COMPLEX

As dicopper alkynyl complexes are implicated as intermediates in the CuAAC reaction, we sought to determine whether **1** would react with an organic azide. Complex **1** serves as a promising model system because of its short Cu–C31 distances (1.953(2) Å), which are similar to those computationally proposed in relevant CuAAC intermediates and transition states.<sup>31,44</sup> In addition, the  $\mu$ - $\eta^1$ : $\eta^1$  binding of the  $\mu$ -alkynyl is similar to the nearly symmetrically bound alkynyl fragments suggested by calculations to form upon interaction of an often dissymmetric ( $\mu$ - $\eta^1$ : $\eta^2$ ) dicopper alkynyl complex with an organic azide.<sup>30,31,44–46,55</sup>

A solution of **1** and *p*-tolylazide (10 equiv) was heated at 60 °C for 23 h in THF, resulting in a color change from green to orange. The <sup>1</sup>H NMR spectrum of the primary product in nitrobenzene-*d*<sub>5</sub> at 24 °C revealed a loss in symmetry between the side arm pyridines, while the symmetry of the naphthyridine rings remained intact. This partial loss of symmetry suggested formation of a bridging triazolide complex, [Cu<sub>2</sub>( $\mu$ - $\eta^1$ : $\eta^1$ -(1,4-bis(4-tolyl)-1,2,3-triazolide))DPFN]NTf<sub>2</sub> (**2**, eq 2), which was isolated in 62% yield. The triazolide



complex was also generated in *o*-C<sub>6</sub>H<sub>4</sub>F<sub>2</sub>, with 77% yield (92% conversion, yield and conversion by <sup>19</sup>F NMR spectroscopy) after treatment of **1** with *p*-tolylazide (10 equiv) and heating for 11.5 h at 60 °C (Figure S8). Similar, but significantly slower, reactivity was observed at room temperature, with 77% yield and 99% conversion after 9.2 days (by <sup>19</sup>F NMR spectroscopy; Figure S9).

Layering hexanes onto a nitrobenzene solution of **2** afforded X-ray quality crystals, and the solid-state structure confirmed formation of a  $\mu$ -triazolide ligand and revealed that the 5-position of the 1,2,3-triazolide nearly symmetrically bridges the two copper centers (Figures 3 and SC2). Ostensibly to accommodate the sterically demanding bridging triazolide ligand, the complex's core structure is significantly expanded compared to those of the  $\mu$ -Ph and  $\mu$ -alkynyl complexes. For example, the Cu–C distances of 2.046(2) and 2.002(2) Å are longer than those observed in **1**. The Cu...Cu distance (2.4139(5) Å) is also longer than those observed in the aforementioned complexes ( $\mu$ -Ph: 2.3927(5) Å,  $\mu$ -alkynyl: 2.3885(4) Å), as are the Cu–N(naphthyridine) bond lengths (2.147(2) and 2.135(2) Å in **2**, compared to 2.095(2) and 2.074(2) Å in the  $\mu$ -Ph complex and 2.075(3)–2.086(3) Å in

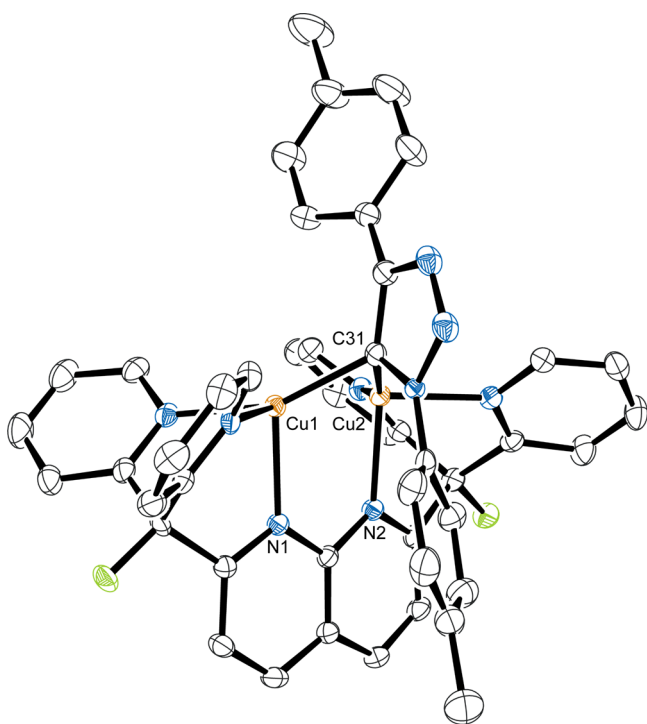


**Figure 3.** Solid-state structure of **2** as determined by single-crystal X-ray diffraction. One  $\text{NTf}_2^-$  counterion and hydrogen atoms are omitted for clarity. Thermal ellipsoids are set at the 50% probability level.

the  $\mu$ -alkynyl complex). While the triazolide binds to the two Cu centers similarly, unlike the bridging aryl<sup>48</sup> and alkynyl ligands, it tilts significantly to one side of the naphthyridine. This tilt accompanies a splaying of the side arm pyridine groups closest to the triazolide, suggesting the distortion results from the steric effects of the bulky triazolide ligand.

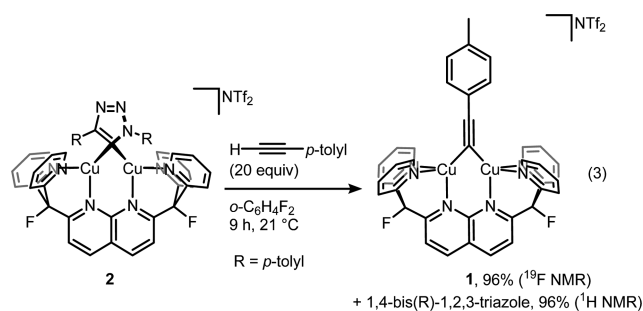
At 24 °C, the  $^1\text{H}$  NMR spectrum of **2** in nitrobenzene- $d_5$  exhibits only two naphthyridine proton resonances, while the  $^{19}\text{F}$  NMR spectrum contains one ligand-assignable fluorine resonance, indicating that in solution, the two copper centers are equivalent on the NMR time scale. This structure is consistent with recent computational studies that predict symmetrical bridging of a triazolide via the C5 position between two copper centers to be a low-energy intermediate in the CuAAC mechanism,<sup>30,31,45,46</sup> as opposed to direct formation of a mononuclear copper triazolide or an unsymmetrically metalated triazolide. Recently, Jin and co-workers reported another dicopper triazolide complex, (1-( $\text{CH}_2\text{C}_6\text{H}_5$ )-4-( $\text{C}_6\text{H}_5$ )-3,5-bis( $\text{CuL}$ )-1,2,3-triazolide,  $\text{L} = 2,2$ -diethyl-4,4-dimethyl-5-( $N$ -2,6-diisopropylphenyl)-cyclic(alkyl) (amino)-carbene), which possesses a solid-state structure in which the 1,2,3-triazolide ligand is bound to the copper atoms at the 3 and 5 positions (Chart 1, H), rather than only at the 5 position.<sup>39</sup> In contrast to **2**, in solution at 25 °C, the two copper centers in the 3,5-bis(metalated) triazolide are reported to be inequivalent on the NMR time scale, as determined by distinct carbene ligand resonances for each.

While cycloadditions have been directly observed with mononuclear copper alkynyl complexes supported by an N-heterocyclic carbene ligand,<sup>32,40</sup> and for a  $\mu$ - $\eta^1$ : $\eta^2$ -dicopper alkynyl complex supported by cyclic (alkyl) (amino)carbenes,<sup>39</sup> a dicopper pathway that includes a symmetrically bridging triazolide is proposed to be a more relevant catalytic manifold

(*vide supra*).<sup>31,40</sup> Thus, the observed alkynyl–azide cycloaddition between **1** and *p*-tolylazide could represent a fundamental step in the dicopper CuAAC reaction pathway.

To investigate the cycloaddition mechanism, the reaction order in both reactants was determined by following the reactions *in situ* by  $^{19}\text{F}$  NMR spectroscopy. Upon addition of 10 equiv of *p*-tolylazide and heating to 60 °C, **1** converted to **2** with a reaction profile consistent with first-order kinetics (Figures S10–11), suggesting that the reaction is first order in **1**. The observed rate constants ( $k_{\text{obs}}$ ) of reactions with *p*-tolylazide concentrations varied between 10 and 100 equiv give a linear dependence on the azide concentration (Figures S12–13), and a plot of  $\ln(k_{\text{obs}})$  vs  $\ln(\text{azide concentration})$  gave a line with a slope of 0.90 (Figure S14). These results strongly suggest that the major reaction is also first order in *p*-tolylazide. Combined, the kinetic studies suggest a bimolecular reaction between the symmetric dicopper  $\mu$ -alkynyl complex and *p*-tolylazide yields the  $\mu$ -triazolide, which is consistent with aforementioned computationally proposed mechanisms.

To determine whether the dicopper triazolide would react with a terminal acetylene, **2** was treated with 20 equiv of *p*-tolylacetylene in *o*- $\text{C}_6\text{H}_4\text{F}_2$ . After 9 h at 22 °C, protodemetalation was nearly complete, yielding **1** in 96% yield (by  $^{19}\text{F}$  NMR spectroscopy) as well as 1,4-bis(4-tolyl)-1,2,3-triazole, also in 96% yield (by  $^1\text{H}$  NMR spectroscopy) (eq 3 and Figure S15).



Given that the established, stoichiometric processes of eqs 2 and 3 seem to represent a viable catalytic mechanism, the efficiency of **1** as a catalyst for CuAAC was investigated. Addition of 10 mol % of **1** to an equimolar solution of *p*-tolylacetylene and *p*-tolylazide in *o*- $\text{C}_6\text{H}_4\text{F}_2$ , and heating to 100 °C for 5.3 h, produced 1,4-bis(4-tolyl)-1,2,3-triazole in 90% yield (by  $^1\text{H}$  NMR spectroscopy, Figure S16). No significant catalyst decomposition was observed by  $^1\text{H}$  NMR spectroscopy (Figure S17). For comparison, heating an equimolar mixture of *p*-tolylacetylene and *p*-tolylazide in *o*- $\text{C}_6\text{H}_4\text{F}_2$  at 100 °C without **1** gave a mixture that contained only 1% yield of the 1,2,3-triazole after 10 h and 9% after 5 days (by  $^1\text{H}$  NMR spectroscopy). Observation of a catalyst turnover number of approximately 9 over the course of 5.3 h at 100 °C is consistent with the rate of stoichiometric cycloaddition with 10 equiv of *p*-tolylazide at 60 °C.

## MIXED-VALENCE DICOPPER(I,II) COMPLEXES

Recent discovery of persistent mixed-valence  $\mu$ -aryl dicopper(I,II) complexes and hypotheses concerning the possible intermediacy of mixed-valence dicopper complexes in the CuAAC reaction<sup>37</sup> prompted a study of the electrochemistry of **1** and **2**. A mixed-valence  $\text{Cu}_2(\text{I,II})$  complex has been hypothesized to be highly efficient in catalysis, since the more

Lewis acidic Cu(II) site could enhance activation of the azide substrate.<sup>37</sup> Notably, upon oxidation of the analogous  $\mu$ -Ph complex, a significant geometric difference between the two copper centers was revealed, with the  $\pi$ -system of the aryl ring ostensibly interacting with the Cu(I) center, while the *ipso*-carbon binds more directly to the Cu(II) center.<sup>48</sup> A similar structure for a mixed-valence  $\mu$ -alkynyl complex could potentially result in higher reactivity toward an organic azide.

Cyclic voltammetry of a solution of **1** revealed a single reversible oxidation–reduction process at  $E^{o'} = 0.022$  V vs  $[\text{Cp}_2\text{Fe}]^{0/1+}$  ( $i_{pa}/i_{pc} = 1.04$ ,  $\Delta E_p = 78$  mV, Figures 4a and S18).

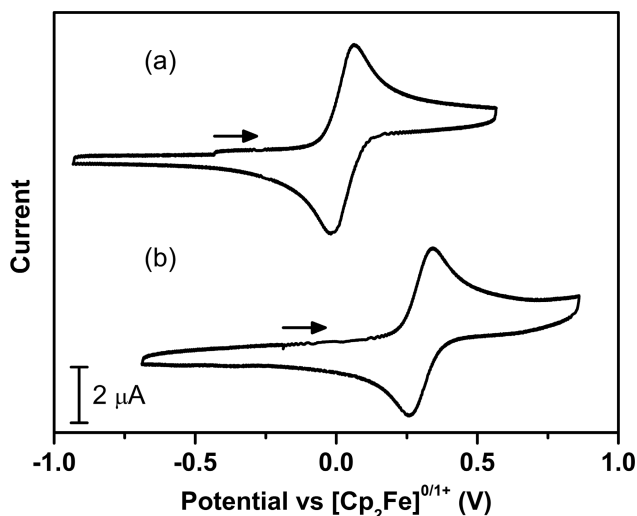


**Figure 4.** Cyclic voltammograms of 0.5 mM solutions of (a) **1** and (b) **2** in *o*-C<sub>6</sub>H<sub>4</sub>F<sub>2</sub> with 0.1 M [nBu<sub>4</sub>N][PF<sub>6</sub>] supporting electrolyte. The arrows indicate the initial potentials and scanning directions. Scan rate: 100 mV/s.

Similarly, cyclic voltammetry of a solution of **2** revealed a single reversible oxidation–reduction process at  $E^{o'} = 0.302$  V vs  $[\text{Cp}_2\text{Fe}]^{0/1+}$  ( $i_{pa}/i_{pc} = 1.16$ ,  $\Delta E_p = 81$  mV, Figures 4b and S22). The redox events observed for both **1** and **2** remain reversible over a range of scan rates, from 10 to 1000 mV/s (Figures S19–20 and S23–24) and are bounded by irreversible oxidation and reduction features (Figures S21 and S25). The higher oxidation potential for **2** is likely due to the electron-withdrawing nature of the triazolide ligand and is consistent with higher oxidation potentials observed for increasingly electron-withdrawing  $\mu$ -aryl groups.<sup>48</sup>

To enable investigation of the mixed-valence complexes in CuAAC catalysis, the synthesis of a mixed-valence  $\mu$ -alkynyl complex was pursued. While the  $\mu$ -Ph complex is oxidized with AgNTf<sub>2</sub>, this oxidant did not cleanly oxidize **1**. However, 1.02 equiv of acetylferrocenium triflimide ([AcFc]<sup>+</sup>NTf<sub>2</sub><sup>-</sup>) reacted with **1** to give [Cu<sub>2</sub>( $\mu$ - $\eta^1$ : $\eta^1$ -C $\equiv$ C(C<sub>6</sub>H<sub>4</sub>)CH<sub>3</sub>)DPFN](NTf<sub>2</sub>)<sub>2</sub> (**3**), which was isolated in 85% yield (eq 4).

Vapor diffusion of diethyl ether into a THF solution of **3** at  $-35$  °C yielded crystals, and X-ray diffraction revealed the solid-state structure (Figure S3). Surprisingly, the mixed-valence  $\mu$ -alkynyl complex exhibits small structural changes to the dicopper core structure (Figure 5, Table 1) relative to those of the oxidized  $\mu$ -Ph complex. Notably, the bending of the  $\mu$ -alkynyl ligand toward one Cu center is not nearly as pronounced as is the bending in the Cu<sub>2</sub>(I,II)  $\mu$ -Ph complex. The  $\angle$ C32–C31–Cu angles in **3** are 136.7(3) and 148.8(3)°, deviating only slightly from the range of angles observed in **1**

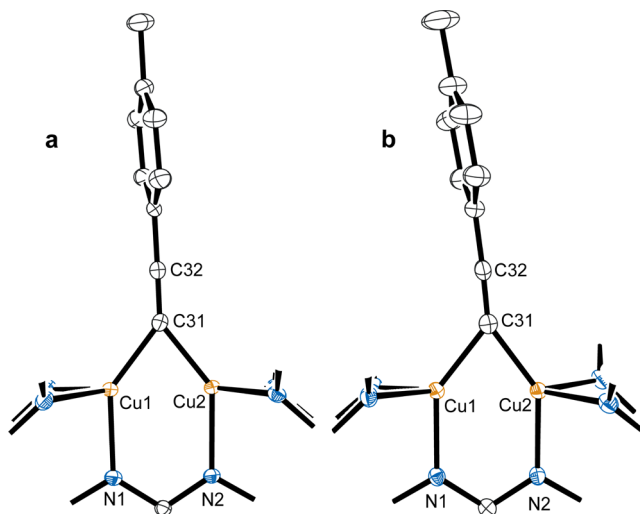
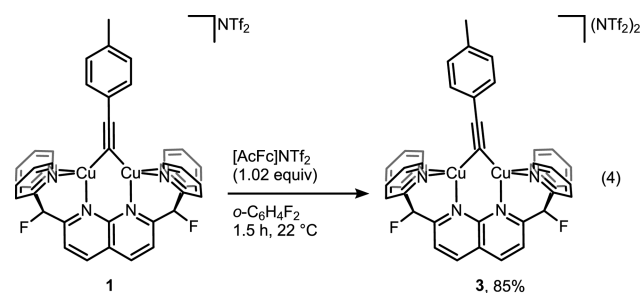


**Figure 5.** Solid-state structures of the cores of (a) **1** and (b) **3** as determined by single-crystal X-ray diffraction. Thermal ellipsoids are set at the 50% probability level.

**Table 1.** Selected Distances, Bond Lengths, and Angles for the [Cu<sub>2</sub>( $\mu$ - $\eta^1$ : $\eta^1$ -C $\equiv$ C(C<sub>6</sub>H<sub>4</sub>)CH<sub>3</sub>)DPFN]<sup>+/+</sup> Cation and Dication

distance (Å) or angle (°)	cation <sup>a</sup>	dication
Cu···Cu	2.3867(6)	2.3356(4)
Cu1–C31	1.955(3)	1.943(3)
Cu2–C31	1.949(3)	1.916(3)
Cu1–N1	2.075(3)	1.988(3)
Cu2–N2	2.078(3)	1.983(3)
C32–C31–Cu1	140.9(3)	136.7(3)
C32–C31–Cu2	143.8(3)	148.8(3)
C31 $\equiv$ C32	1.222(5)	1.234(5)

<sup>a</sup>Cation metrics for the molecule displayed in Figures 1 and 5.

(140.9(3) to 143.8(3)°). In comparison, oxidation of the  $\mu$ -Ph complex induced a much more significant tilt, with comparable angles changing from 144.4(1) and 143.0(1)° to 119.9(2) and 167.5(3)° upon oxidation. The Cu–C31 distances in **3** remain relatively similar, shortening and diverging from an average of 1.953(2) Å in **1** to 1.943(3) and 1.916(3) Å in **3**. The difference between the Cu–C31 bond lengths (0.027 Å) in **3** is significantly less than that observed in the mixed-valence  $\mu$ -Ph complex (0.137 Å). In addition, the Cu···Cu distance in the  $\mu$ -alkynyl complexes shortened considerably upon oxidation, from 2.3885(4) Å to 2.3356(4) Å (a contraction of 0.053 Å), which is more than the contraction observed upon oxidation of the  $\mu$ -Ph complex (0.012 Å).

The C–C triple bond distance exhibited little change in the solid-state structure with oxidation, lengthening from an

average of 1.217(4) to 1.234(5) Å. However, a more noticeable change was observed in the C≡C IR stretch, which shifted from 2030 cm<sup>-1</sup> in **1** to 1971 cm<sup>-1</sup> in **3**.

The  $\mu$ -Ph complex was found by EPR spectroscopy to exhibit significant spin localization at low temperatures, consistent with its structural desymmetrization in the solid-state, while increased spin delocalization and a more symmetric structure was evidenced in room temperature solution.<sup>48</sup> In contrast, the significantly shortened Cu...Cu distance and only slight desymmetrization between the Cu centers in **3** suggest that the spin might be more delocalized than in the  $\mu$ -Ph analogue. Thus, spectroscopic investigations were pursued to estimate the extent of spin localization. UV-vis-NIR spectroscopy of a solution of **3** in THF revealed a strong band in the NIR that was not present in a solution of **1** (Figure S26). Modeling the region between 6002 and 22,523 cm<sup>-1</sup> as a sum of four Gaussian curves provided a good fit (Figure S27) for the lowest-energy band, which is tentatively assigned as an intervalence charge transfer (IVCT) band. The transition is centered around 10,426 cm<sup>-1</sup> and is slightly lower in energy than the IVCT band of the mixed-valence  $\mu$ -Ph complex (11,086 cm<sup>-1</sup>). The band is also significantly less intense with  $\epsilon_{\text{max}} = 822 \text{ M}^{-1} \text{ cm}^{-1}$  (vs 2478 M<sup>-1</sup> cm<sup>-1</sup> for the  $\mu$ -Ph complex) and narrower with a fwhm of 2908 cm<sup>-1</sup> (vs 3409 cm<sup>-1</sup> for the  $\mu$ -Ph complex). Compared to those observed for other complexes, these band parameters suggest that **3** has at least partial spin-localization, designating it as a Class II complex in the Robin-Day classification scheme.<sup>56-58</sup> Estimating the ground-state delocalization parameter ( $\alpha^2$ ) from the IVCT band parameters gives  $\alpha^2 \approx 0.018$ , which ostensibly suggests that the spin is localized in a manner similar to that of the mixed-valence  $\mu$ -Ph complex ( $\alpha^2 \approx 0.057$ ). However, this result is inconsistent with the small structural changes observed upon oxidizing **1** to **3**, especially in comparison to the significant changes observed upon oxidation of the  $\mu$ -Ph complex.

The classification of dicopper complexes as Class I, II, or III, and the nature of spin localization, can also be addressed with EPR spectroscopy.<sup>48,59-62</sup> Spectra of Class I mixed-valence dicopper complexes typically exhibit four resonances, indicating that the unpaired electron spin ( $S = 1/2$ ) is localized primarily on one Cu(II) ion (nuclear spin  $I = 3/2$ ).<sup>60,63-65</sup> In contrast, spectra of Class III dicopper complexes commonly display seven peaks, suggesting equal delocalization across both copper centers on the EPR time scale.<sup>66-71</sup> Between these extremes, Class II complexes are often identified by the temperature dependence of their EPR spectra, with four peaks observed at lower temperatures and seven at high temperatures.<sup>59,60,72,73</sup>

The extent of spin localization of **3** was more directly investigated with continuous-wave (cw) X-band EPR spectroscopy. The EPR spectra of a frozen solution of **3** in THF exhibited a rhombic signal with at least seven peaks at  $g \approx 2$ , and the line-shape splittings remained consistent between 30 and 130 K (Figure S28). The appearance of more than four peaks attributable to hyperfine interactions with the nuclear spins on both Cu centers, and their persistence down to 30 K, suggests that the spin is more delocalized between the two metal centers than in the mixed valence  $\mu$ -Ph complex, which exhibited four distinct peaks at low temperatures. However, the spectrum does not resemble those reported for many Class III complexes, in which seven hyperfine peaks are easily discernible.<sup>62,66,68-71,74-79</sup> The EPR spectra observed for **3** are similar to those observed for a series of half-met hemocyanins as reported by Westmoreland et al.<sup>61,80</sup> The

half-met-L dicopper sites were found to be Class II, with the extent of spin delocalization dependent on the geometry and exogenous ligand.

Taken together, the spectral similarity to the half-met-L dicopper sites and the slight structural differentiation between the two copper centers suggest that **3** might be a Class II complex that exhibits delocalization of the electron spin, even at low temperatures. A spectral simulation of an electron spin with electron-nuclear hyperfine interactions with inequivalent Cu centers provided a good fit of the experimental spectrum obtained for **3** in THF at 110 K (Figure 6). The  $g$  values and

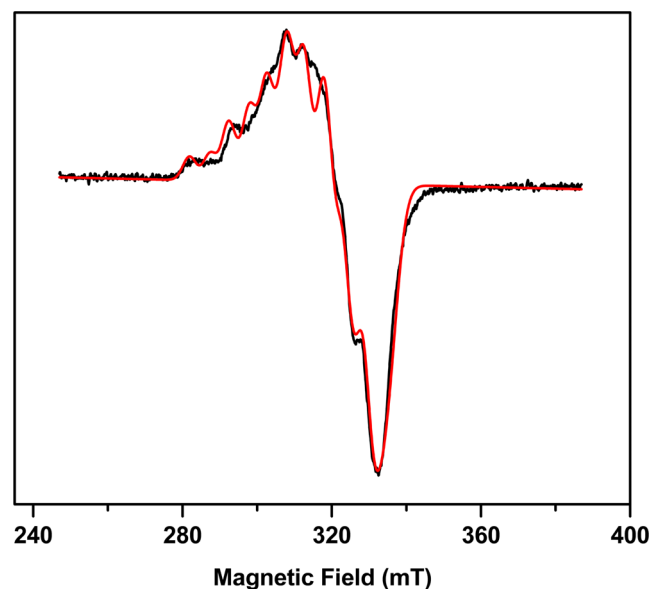


**Figure 6.** Experimental (black trace) and simulated (red trace) cw EPR spectra of **3** in THF at 110 K. The numerical simulation was obtained with  $g$  values of  $g_1 = 2.044$ ,  $g_2 = 2.107$ ,  $g_3 = 2.194$  and principal hyperfine components of  $A_1^{\text{Cu1}} = 36.1$ ,  $A_2^{\text{Cu1}} = 49.0$ ,  $A_3^{\text{Cu1}} = 102.7 \times 10^{-4} \text{ T}$  and  $A_1^{\text{Cu2}} = 6.8$ ,  $A_2^{\text{Cu2}} = 12.2$ ,  $A_3^{\text{Cu2}} = 56.4 \times 10^{-4} \text{ T}$ .

hyperfine interaction parameters employed in the simulation are consistent with those reported for other Class II dicopper complexes,<sup>60,73</sup> and especially with the half-met-Br<sup>-</sup> and -I<sup>-</sup> hemocyanin dicopper sites.<sup>61</sup> The highly anisotropic and different Cu1 and Cu2 hyperfine parameters obtained from the simulations suggest that the distribution of the electron spin density on the two copper centers is slightly inequivalent. Taken together with the structure determined by X-ray crystallography, the EPR spectra and the hyperfine coupling parameters estimated by spectral simulation indicate a greater extent of spin delocalization than is estimated by analysis of the IVCT band. As was also observed by Westmoreland et al., analysis of the optical band parameters appears to underestimate the degree of spin delocalization observed.<sup>61</sup>

The nature of **3** in solution at room temperature was examined with <sup>19</sup>F NMR spectroscopy. In *o*-C<sub>6</sub>H<sub>4</sub>F<sub>2</sub> at 296 K, two fluorine resonances are observed, at -78.79 ppm and -176.40 ppm (vs CFCl<sub>3</sub>, Figure S29). As with the mixed-valence  $\mu$ -Ph complex, integration suggests the former resonance can be assigned to the triflimide anions (NTf<sub>2</sub><sup>-</sup>), while the latter can be assigned to the dication. The dication resonance's appearance as a broad singlet is consistent with equivalence of the two Cu centers in **3** on the NMR time scale, which is expected as little geometric change was observed in the solid state and significant delocalization was observed by EPR

even at low temperatures, further supporting the assignment of **3** as a Class II mixed-valence complex.

To probe the effect of the dicopper core's electronic structure on its cycloaddition reactivity, **3** was treated with *p*-tolylazide (10 equiv) in *o*-C<sub>6</sub>H<sub>4</sub>F<sub>2</sub>, and the resulting solution was heated to 60 °C. While approximately 1 equiv of *p*-tolylazide was consumed over the course of the first 8.7 h, decomposition of **3** into a range of products was observed. Decomposition was evidenced by the appearance of <sup>1</sup>H and <sup>19</sup>F NMR resonances also observed upon heating **3** in *o*-C<sub>6</sub>H<sub>4</sub>F<sub>2</sub> in the absence of *p*-tolylazide (Figures S30–31). Addition of isopropylacetylene to the reaction mixture revealed that 1,4-bis(4-tolyl)-1,2,3-triazole had formed among a mixture of products (determined by <sup>1</sup>H NMR spectroscopy). Similar, albeit slower, decomposition of **3** was observed upon treating **3** with *p*-tolylazide (10 equiv) and allowing the mixture to stand at room temperature (Figure S32). (The fate of the acetylide upon heating **3** in the absence of *p*-tolylazide for 2 d remains unknown; di-*p*-tolylbutadiyne was not observed by <sup>1</sup>H NMR spectroscopy or GCMS.)

In comparison to the decomposition observed upon attempting to monitor cycloaddition of **3** with *p*-tolylazide, **1** persists under cycloaddition conditions (*vide supra*). This difference in reactivity suggests that the competent catalyst in CuAAC is likely a dicopper complex with both metal centers in the +1 oxidation state.

## CONCLUDING REMARKS

These results demonstrate that a dicopper complex with a symmetrically bridging,  $\mu$ -alkynyl ligand undergoes cycloaddition with an organic azide to yield a symmetrically bridged 1,2,3-triazolide, where both copper centers bind to the C-5 position of the ring. This reaction embodies a key step that has been postulated in computationally proposed mechanisms of the CuAAC reaction<sup>30,31,45,46</sup> and allows structural characterization of the predicted intermediate. To complete the proposed catalytic cycle, the resulting triazolide reacts with a terminal alkyne to regenerate the  $\mu$ -alkynyl dicopper complex. Moreover, the  $\mu$ -alkynyl dicopper complex is a competent catalyst for the CuAAC reaction.

Both the  $\mu$ -alkynyl and  $\mu$ -triazolide dicopper complexes exhibit reversible one-electron oxidation events. Along with a previously reported hypothesis,<sup>37</sup> these results suggested that the CuAAC could potentially proceed through mixed-valence dicopper complexes. Synthesis of the mixed-valence  $\mu$ -alkynyl complex allowed investigation of its structure and electronic state, revealing a significantly more symmetric dicopper core than was observed upon one-electron oxidation of a related  $\mu$ -phenyl complex. This more symmetric core is consistent with an increased degree of spin delocalization, as evidenced by EPR spectroscopy. Finally, studies of the reactivity of the mixed-valence  $\mu$ -alkynyl complex with *p*-tolylazide show that decomposition of the complex significantly competes with cycloaddition, under conditions that lead to cycloaddition with the corresponding Cu<sub>2</sub>(I,I) complex.

This work furthers the investigation of discrete cationic dicopper complexes exhibiting symmetrically bridging organic ligands and their mixed-valence derivatives. We expect that these compounds will continue to be useful for the discovery of new reactivity, development of reagents, and elucidation of mechanisms that may involve mixed-valence organocopper species. Moreover, a better mechanistic understanding of dicopper intermediates in CuAAC will hopefully inform efforts

to develop increasingly efficient catalysts and broaden the reaction's application to systems where copper concentrations must be minimized and catalysts controlled to avoid toxicity.<sup>12,16,81–83</sup>

## ASSOCIATED CONTENT

### Supporting Information

The Supporting Information is available free of charge on the ACS Publications website at DOI: 10.1021/jacs.6b13261.

SC1: X-ray crystallographic data for **1**·2(C<sub>6</sub>H<sub>3</sub>F) (CIF)

SC2: X-ray crystallographic data for **2** (CIF)

SC3: X-ray crystallographic data for **3**·(C<sub>4</sub>H<sub>10</sub>O) (CIF)

CIF files can also be obtained free of charge from the Cambridge Crystallographic Data Centre under reference numbers 1524417, 1524418, 1524419.

Experimental details, supplementary figures and tables, and crystallographic figures and data (PDF)

## AUTHOR INFORMATION

### Corresponding Author

\*tdtilley@berkeley.edu

### ORCID

Micah S. Ziegler: 0000-0002-8549-506X

### Notes

The authors declare no competing financial interest.

## ACKNOWLEDGMENTS

This work was primarily funded by the U.S. Department of Energy, Office of Science, Office of Basic Energy Sciences, Chemical Sciences, Geosciences, and Biosciences Division under contract no. DE-AC02-05CH11231 (T.D.T.). The EPR investigations were funded by the DOE Office of Science, Office of Basic Energy Sciences, Chemical Sciences, Geosciences, and Biosciences Division, under contract no. DE-FG02-07ER15903 (K.V.L.). We acknowledge the National Institutes of Health (NIH) for funding the UC Berkeley CheXray X-ray crystallographic facility under grant no. S10-RR027172 and the UC Berkeley College of Chemistry NMR facility under grant nos. SRR023679A and 1S10RR016634-01 as well as the Joint Center for Artificial Photosynthesis, a U.S. Department of Energy, Office of Science, Basic Energy Sciences Innovation Hub, under grant no. DE-SC0004993, for EPR facilities. Funds for the QB3 900 MHz NMR spectrometer were provided by the NIH through grant no. GM68933. In addition, M.S.Z. was supported by a National Science Foundation (NSF) Graduate Research Fellowship (grant no.: DGE 1106400) and a Philomathia Graduate Fellowship in the Environmental Sciences. We thank Prof. Robert G. Bergman, Prof. Richard A. Andersen, Dr. Daniel S. Levine, Dr. Allegra L. Liberman-Martin, Amélie Nicolay, Ioannis Mountziaris, Stephen von Kugelgen, Dr. Timothy C. Davenport, Eva Nichols, Dr. Hsueh-Ju Liu, and Tobias F. Sjolander for useful conversations. In addition, we thank Dr. Michael L. Aubrey for electrochemical equipment and Philip C. Bunting for assistance with UV–vis–NIR spectroscopy. Finally, we thank Dr. Antonio G. DiPasquale for X-ray crystallography advice and Dr. Hasan Celik and Dr. Jeffrey G. Pelton for NMR spectroscopy advice.

## REFERENCES

(1) L'abbé, G.; Mahy, M.; Bollyn, M.; Germain, G.; Scheefer, G. *Bull. Soc. Chim. Belg.* **1983**, *92*, 881.



- (2) L'abbé, G. *Bull. Soc. Chim. Belg.* **1984**, *93*, 579.
- (3) Tornøe, C. W.; Christensen, C.; Meldal, M. *J. Org. Chem.* **2002**, *67*, 3057.
- (4) Rostovtsev, V. V.; Green, L. G.; Fokin, V. V.; Sharpless, K. B. *Angew. Chem., Int. Ed.* **2002**, *41*, 2596.
- (5) Kolb, H. C.; Finn, M. G.; Sharpless, K. B. *Angew. Chem., Int. Ed.* **2001**, *40*, 2004.
- (6) Wang, Q.; Chan, T. R.; Hilgraf, R.; Fokin, V. V.; Sharpless, K. B.; Finn, M. G. *J. Am. Chem. Soc.* **2003**, *125*, 3192.
- (7) Kolb, H. C.; Sharpless, K. B. *Drug Discovery Today* **2003**, *8*, 1128.
- (8) Goodall, G. W.; Hayes, W. *Chem. Soc. Rev.* **2006**, *35*, 280.
- (9) Binder, W. H.; Sachsenhofer, R. *Macromol. Rapid Commun.* **2007**, *28*, 15.
- (10) Lutz, J.-F. *Angew. Chem., Int. Ed.* **2007**, *46*, 1018.
- (11) Hawker, C. J.; Fokin, V. V.; Finn, M. G.; Sharpless, K. B. *Aust. J. Chem.* **2007**, *60*, 381.
- (12) Moses, J. E.; Moorhouse, A. D. *Chem. Soc. Rev.* **2007**, *36*, 1249.
- (13) Meldal, M. *Macromol. Rapid Commun.* **2008**, *29*, 1016.
- (14) Meldal, M.; Tornøe, C. W. *Chem. Rev.* **2008**, *108*, 2952.
- (15) Finn, M. G.; Fokin, V. V. *Chem. Soc. Rev.* **2010**, *39*, 1231.
- (16) Schoffelen, S.; Meldal, M. In *Modern Alkyne Chemistry*; Trost, B. M., Li, C.-J., Eds.; Wiley-VCH Verlag GmbH & Co. KGaA: Weinheim, Germany, 2014; pp 113–142.
- (17) Castro, V.; Rodríguez, H.; Albericio, F. *ACS Comb. Sci.* **2016**, *18*, 1.
- (18) Chassaing, S.; Bénétteau, V.; Pale, P. *Catal. Sci. Technol.* **2016**, *6*, 923.
- (19) Himo, F.; Lovell, T.; Hilgraf, R.; Rostovtsev, V. V.; Noodleman, L.; Sharpless, K. B.; Fokin, V. V. *J. Am. Chem. Soc.* **2005**, *127*, 210.
- (20) Rodionov, V. O.; Fokin, V. V.; Finn, M. G. *Angew. Chem., Int. Ed.* **2005**, *44*, 2210.
- (21) Bock, V. D.; Hiemstra, H.; van Maarseveen, J. H. *Eur. J. Org. Chem.* **2006**, *2006*, 51.
- (22) Rodionov, V. O.; Presolski, S. I.; Gardinier, S.; Lim, Y.-H.; Finn, M. G. *J. Am. Chem. Soc.* **2007**, *129*, 12696.
- (23) Rodionov, V. O.; Presolski, S. I.; Díaz Díaz, D.; Fokin, V. V.; Finn, M. G. *J. Am. Chem. Soc.* **2007**, *129*, 12705.
- (24) Presolski, S. I.; Hong, V.; Cho, S.-H.; Finn, M. G. *J. Am. Chem. Soc.* **2010**, *132*, 14570.
- (25) Hein, J. E.; Fokin, V. V. *Chem. Soc. Rev.* **2010**, *39*, 1302.
- (26) Buckley, B. R.; Heaney, H. In *Click Triazoles*, Topics in Heterocyclic Chemistry; Košmrlj, J., Ed.; Springer: Berlin, Germany, 2012; pp 1–29.
- (27) Berg, R.; Straub, B. F. *Beilstein J. Org. Chem.* **2013**, *9*, 2715.
- (28) Ikhlef, D.; Wang, C.; Kahlal, S.; Maouche, B.; Astruc, D.; Saillard, J.-Y. *Comput. Theor. Chem.* **2015**, *1073*, 131.
- (29) Wang, C.; Ikhlef, D.; Kahlal, S.; Saillard, J.-Y.; Astruc, D. *Coord. Chem. Rev.* **2016**, *316*, 1.
- (30) Kalvet, I.; Tammiku-Taul, J.; Mäeorg, U.; Tamm, K.; Burk, P.; Sikk, L. *ChemCatChem* **2016**, *8*, 1804.
- (31) Özkılıç, Y.; Tüzün, N. Ş. *Organometallics* **2016**, *35*, 2589.
- (32) Nolte, C.; Mayer, P.; Straub, B. F. *Angew. Chem., Int. Ed.* **2007**, *46*, 2101.
- (33) Buckley, B. R.; Dann, S. E.; Harris, D. P.; Heaney, H.; Stubbs, E. C. *Chem. Commun.* **2010**, *46*, 2274.
- (34) Buckley, B. R.; Dann, S. E.; Heaney, H. *Chem. - Eur. J.* **2010**, *16*, 6278.
- (35) Makarem, A.; Berg, R.; Rominger, F.; Straub, B. F. *Angew. Chem., Int. Ed.* **2015**, *54*, 7431.
- (36) Díez-González, S. In *Advances in Organometallic Chemistry*; Pérez, P. J., Ed.; Academic Press: Cambridge, MA, 2016; Vol. 66, pp 93–141.
- (37) Kuang, G.-C.; Guha, P. M.; Brotherton, W. S.; Simmons, J. T.; Stanke, L. A.; Nguyen, B. T.; Clark, R. J.; Zhu, L. *J. Am. Chem. Soc.* **2011**, *133*, 13984.
- (38) Berg, R.; Straub, J.; Schreiner, E.; Mader, S.; Rominger, F.; Straub, B. F. *Adv. Synth. Catal.* **2012**, *354*, 3445.
- (39) Jin, L.; Tolentino, D. R.; Melaimi, M.; Bertrand, G. *Sci. Adv.* **2015**, *1*, e1500304.
- (40) Worrell, B. T.; Malik, J. A.; Fokin, V. V. *Science* **2013**, *340*, 457.
- (41) Iacobucci, C.; Reale, S.; Gal, J.-F.; De Angelis, F. *Angew. Chem., Int. Ed.* **2015**, *54*, 3065.
- (42) Iacobucci, C.; Lebon, A.; De Angelis, F.; Memboeuf, A. *Chem. - Eur. J.* **2016**, *22*, 18690.
- (43) Jin, L.; Romero, E. A.; Melaimi, M.; Bertrand, G. *J. Am. Chem. Soc.* **2015**, *137*, 15696.
- (44) Ahlquist, M.; Fokin, V. V. *Organometallics* **2007**, *26*, 4389.
- (45) Straub, B. F. *Chem. Commun.* **2007**, No. 37, 3868.
- (46) Cantillo, D.; Ávalos, M.; Babiano, R.; Cintas, P.; Jiménez, J. L.; Palacios, J. C. *Org. Biomol. Chem.* **2011**, *9*, 2952.
- (47) Zhu, L.; Brassard, C. J.; Zhang, X.; Guha, P. M.; Clark, R. J. *Chem. Rec.* **2016**, *16*, 1501.
- (48) Ziegler, M. S.; Levine, D. S.; Lakshmi, K. V.; Tilley, T. D. *J. Am. Chem. Soc.* **2016**, *138*, 6484.
- (49) van Koten, G.; Jastrzebski, J. T. B. H. In *PATAI'S Chemistry of Functional Groups*; John Wiley & Sons, Ltd: Chichester, U.K., 2009.
- (50) Lang, H.; Jakob, A.; Milde, B. *Organometallics* **2012**, *31*, 7661.
- (51) Reger, D. L.; Collins, J. E.; Huff, M. F.; Rheingold, A. L.; Yap, G. P. A. *Organometallics* **1995**, *14*, 5475.
- (52) Kuang, S.-M.; Zhang, Z.-Z.; Wang, Q.-G.; Mak, T. C. W. *J. Chem. Soc., Dalton Trans.* **1998**, No. 7, 1115.
- (53) Wyss, C. M.; Bitting, J.; Bacsa, J.; Gray, T. G.; Sadighi, J. P. *Organometallics* **2016**, *35*, 71.
- (54) Dawson, D. A.; Reynolds, W. F. *Can. J. Chem.* **1975**, *53*, 373.
- (55) Calvo-Losada, S.; Pino-González, M. S.; Quirante, J. J. *J. Phys. Chem. B* **2015**, *119*, 1243.
- (56) D'Alessandro, D. M.; Keene, F. R. *Chem. Rev.* **2006**, *106*, 2270.
- (57) Robin, M. B.; Day, P. In *Advances in Inorganic Chemistry and Radiochemistry*; Emeléus, H. J., Sharpe, A. G., Eds.; Academic Press: Cambridge, MA, 1968; Vol. 10, pp 247–422.
- (58) Allen, G. C.; Hush, N. S. In *Progress in Inorganic Chemistry*; Cotton, F. A., Ed.; John Wiley & Sons, Inc.: Hoboken, NJ, 1967; pp 357–389.
- (59) Gagne, R. R.; Koval, C. A.; Smith, T. J. *J. Am. Chem. Soc.* **1977**, *99*, 8367.
- (60) Long, R. C.; Hendrickson, D. N. *J. Am. Chem. Soc.* **1983**, *105*, 1513.
- (61) Westmoreland, T. D.; Wilcox, D. E.; Baldwin, M. J.; Mims, W. B.; Solomon, E. I. *J. Am. Chem. Soc.* **1989**, *111*, 6106.
- (62) Jeffery, J. C.; Riis-Johannessen, T.; Anderson, C. J.; Adams, C. J.; Robinson, A.; Argent, S. P.; Ward, M. D.; Rice, C. R. *Inorg. Chem.* **2007**, *46*, 2417.
- (63) Addison, A. W. *Inorg. Nucl. Chem. Lett.* **1976**, *12*, 899.
- (64) Mandal, S. K.; Thompson, L. K.; Nag, K.; Charland, J. P.; Gabe, E. J. *Inorg. Chem.* **1987**, *26*, 1391.
- (65) Srinivas, B.; Zacharias, P. S. *Polyhedron* **1992**, *11*, 1949.
- (66) Barr, M. E.; Smith, P. H.; Antholine, W. E.; Spencer, B. J. *Chem. Soc., Chem. Commun.* **1993**, *21*, 1649.
- (67) LeCloux, D. D.; Davydov, R.; Lippard, S. J. *J. Am. Chem. Soc.* **1998**, *120*, 6810.
- (68) Harding, C.; Nelson, J.; Symons, M. C. R.; Wyatt, J. J. *Chem. Soc., Chem. Commun.* **1994**, No. 21, 2499.
- (69) He, C.; Lippard, S. J. *Inorg. Chem.* **2000**, *39*, 5225.
- (70) Gupta, R.; Zhang, Z. H.; Powell, D.; Hendrich, M. P.; Borovik, A. S. *Inorg. Chem.* **2002**, *41*, 5100.
- (71) Hagadorn, J. R.; Zahn, T. I.; Lawrence Que, J.; Tolman, W. B. *Dalton Trans.* **2003**, No. 9, 1790.
- (72) Gagne, R. R.; Koval, C. A.; Smith, T. J.; Cimolino, M. C. *J. Am. Chem. Soc.* **1979**, *101*, 4571.
- (73) Tandon, S. S.; Thompson, L. K.; Bridson, J. N. *Inorg. Chem.* **1993**, *32*, 32.
- (74) Sigwart, C.; Hemmerich, P.; Spence, J. T. *Inorg. Chem.* **1968**, *7*, 2545.
- (75) Mandal, S. K.; Thompson, L. K.; Newlands, M. J.; Gabe, E. J. *Inorg. Chem.* **1989**, *28*, 3707.
- (76) Houser, R. P.; Young, V. G.; Tolman, W. B. *J. Am. Chem. Soc.* **1996**, *118*, 2101.

- (77) LeCloux, D. D.; Davydov, R.; Lippard, S. J. *Inorg. Chem.* **1998**, *37*, 6814.
- (78) Harkins, S. B.; Peters, J. C. *J. Am. Chem. Soc.* **2004**, *126*, 2885.
- (79) McMoran, E. P.; Powell, D. R.; Perez, F.; Rowe, G. T.; Yang, L. *Inorg. Chem.* **2016**, *55*, 11462.
- (80) Solomon, E. I.; Gewirth, A. A.; Westmoreland, T. D. In *Advanced EPR*; Hoff, A. J., Ed.; Elsevier: Amsterdam, 1989; pp 865–908.
- (81) Hong, V.; Steinmetz, N. F.; Manchester, M.; Finn, M. G. *Bioconjugate Chem.* **2010**, *21*, 1912.
- (82) Lallana, E.; Riguera, R.; Fernandez-Megia, E. *Angew. Chem., Int. Ed.* **2011**, *50*, 8794.
- (83) Uttamapinant, C.; Tangpeerachaikul, A.; Grecian, S.; Clarke, S.; Singh, U.; Slade, P.; Gee, K. R.; Ting, A. Y. *Angew. Chem., Int. Ed.* **2012**, *51*, 5852.